



Contents lists available at ScienceDirect

Journal of Biomechanics

journal homepage: www.elsevier.com/locate/jbiomech
www.JBiomech.com

Robotic simulation of identical athletic-task kinematics on cadaveric limbs exhibits a lack of differences in knee mechanics between contralateral pairs

Nathaniel A. Bates^{a,b}, April L. McPhearson^{b,c}, Rebecca J. Nesbitt^b, Jason T. Shearn^b, Gregory D. Myer^{c,e,f,g}, Timothy E. Hewett^{a,b,c,d,e,h,*}

^a Department of Orthopedic Surgery, Mayo Clinic, Rochester, MN, USA

^b Department of Biomedical Engineering, University of Cincinnati, Cincinnati, OH, USA

^c Sports Medicine Biodynamics Center, Division of Sports Cincinnati Children's Hospital Medical Center, Cincinnati, OH, USA

^d The Sports Health and Performance Institute, The Ohio State University, Columbus, OH, USA

^e Department of Pediatrics, College of Medicine, University of Cincinnati, Cincinnati, OH, USA

^f Department of Orthopaedic Surgery, College of Medicine, University of Cincinnati, Cincinnati, OH, USA

^g The Micheli Center for Sports Injury Prevention, Boston, MA, USA

^h Departments of Physiology and Cell Biology, Orthopaedic Surgery, Family Medicine, and Biomedical Engineering, The Ohio State University, Columbus, OH, USA

ARTICLE INFO

Article history:

Accepted 19 December 2016

Keywords:

Knee biomechanics
Contralateral pairs
Side asymmetry
Joint simulation
Robotic knee articulation

ABSTRACT

Limb asymmetry is a known factor for increased ACL injury risk. These asymmetries are normally observed during *in vivo* testing. Prior studies have developed *in vitro* testing methodologies driven by *in vivo* kinematics to investigate knee mechanics relative to ACL injury. The objective of this study was to determine if mechanical side-to-side asymmetries persist in contralateral pairs during *in vitro* simulation testing. *In vivo* kinematics were recorded for male and female drop vertical jump and sidestep cutting tasks. The recorded kinematics were used to robotically simulate the motions on 7 contralateral pairs of cadaveric lower extremities specimens. ACL and MCL force, torque, and strains were recorded and analyzed for differences between contralateral pairs. There was a general lack of mechanical differences between limb sides. Adduction peak torque for the male sidestep cut movement was significantly different between limb sides ($p=0.04$). However, this is consistent with ACL injury mechanics in that movement in the frontal plane (abduction/adduction) increases injury risk and it is possible loading differences in this plane may have resulted from tolerances within the setup process. The findings of this study indicate that contralateral knee joints were representative of each other during biomechanical *in vitro* tests. In future cadaveric robotic simulations, contralateral limbs can be used interchangeably. In addition, direct comparisons of the structural behaviors of isolated conditions for contralateral knee joints can be performed.

© 2017 Elsevier Ltd. All rights reserved.

1. Introduction

There are approximately 250,000 anterior cruciate ligament (ACL) injuries per year in the United States (Johnson and Warner, 1993) and 2 million injuries worldwide (Renstrom, 2013), with each reconstructive procedure estimated at \$17,000 (Hewett et al., 1999). The exact mechanism of ACL injury is difficult to define, since most ACL injuries occur in non-contact situations with movements that involve both rapid deceleration and a change of direction (Boguszewski, 2012; Griffin et al., 2000; McNair et al., 1990; Mei

et al., 2013). *In vivo* biomechanical simulations have identified several factors associated with increased ACL injury risk, including excessive knee valgus, asymmetry, and poor trunk position (Griffin et al., 2000; Griffin et al., 2006; Pappas et al., 2013).

Side-to-side asymmetry is a known risk factor for increased ACL injury (Pappas and Carpes, 2012; Paterno et al., 2007). Some degree of asymmetry is naturally present between dominant and non-dominant legs in a random sample of women independent of athletic participation (Lanshammar and Ribom, 2011). However, leg-to-leg differences in knee joint loading have prospectively been documented to be greater in athletes who went on to ACL injury than those who did not (Hewett et al., 2005). Specifically, those female athletes who later experienced injury had 6.4 times greater side-to-side differences in abduction torque during jump

* Corresponding author at: Department of Orthopedic Surgery, Mayo Clinic, Rochester, MN, USA. Fax: +1 507 284 5392.

E-mail address: hewett.timothy@mayo.edu (T.E. Hewett).

landing than did uninjured athletes. Furthermore, during performance of jump-landing athletic tasks, female subjects, who are known to be at increased risk for ACL injury (Arendt et al., 1999; Boden et al., 2000), exhibited greater measures of side-to-side asymmetry than males (Pappas and Carpes, 2012). Following ACL reconstruction (ACLR), limb asymmetry continues to exist, as 52% of patients who failed to pass return-to-sport criteria 6 months following ACLR were found to have significant side-to-side differences in knee kinematics and kinetics (Di Stasi et al., 2013). In addition, at two years following ACLR, vertical ground reaction force differences exist in jump landing movements between the ACLR-involved limb and both the uninvolved limb and control limbs of non-injured subjects. The presence of limb asymmetries increases an individual's risk for ACL injury (Paterno et al., 2007).

Asymmetry effects on ligament mechanics from previous literature are limited due to their inability to conduct direct, invasive research on a human ACL within an *in vivo* athletic setting. *In vitro* biomechanical simulations, such as robotically-driven knee simulations, provide relevant alternative solutions to compensate for the impracticality of *in vivo* studies. A simulation methodology to directly investigate ACL behavior during athletic tasks by driving cadaveric knee joints through *in vivo* kinematics has been developed (Bates et al., 2015). However, mechanical response between pairs of lower extremity specimens procured from the same donor have not yet been compared.

The objective of this study was to determine whether mechanical side-to-side asymmetries persist in contralateral limb pairs *in vitro* during the robotic simulation of identical kinematics recorded from *in vivo* athletic tasks. The hypothesis tested was that statistically significant side-to-side joint loading asymmetries would be observed during *in vitro* simulations of motion. This was hypothesized as side-to-side asymmetries have previously been identified during *in vivo* motion capture analyses (Hewett et al., 2005).

2. Methods

2.1. Kinematic model

This investigation used *in vivo* recorded kinematics to perform robotic simulations of knee joint articulations during athletic tasks. The methods of robotic simulation applied in the present study have been previously described in the literature (Bates et al., 2015). Briefly, a 10-camera three-dimensional (3D) motion capture system (Eagle cameras, Motion Analysis Corp., Santa Rosa, CA) recorded 3D positional data at 240 Hz on a matched male (age=24 years; height=175 cm; mass=675 N) and female (age=25; height=170 cm; mass=632 N) athlete during drop vertical jump (DVJ) and sidestep cutting athletic tasks (Ford et al., 2003; Ford et al., 2005). The 3D tracking data was then filtered through a fourth-order, low-pass, digital filter at 6 Hz and processed through an established biomechanical model in Visual3D (version 4.0, C-Motion, Inc., Germantown, MD) using custom MATLAB code (version 2012b, The MathWorks, Inc., Natick, MA) to calculate 3D joint kinematics (Ford et al., 2007). Using previously prescribed methods, mathematical factors were applied to reduce the confounding effects of skin-artifact errors on these kinematics which were utilized as input to constrain robotic simulations of knee articulation in cadaveric specimens (Bates et al., 2015).

2.2. Robotic simulations

Fourteen (14) lower extremity cadaveric specimens from seven unique donors (age=47.2 ± 8.9 years; mass=876 ± 201 N; BMI=29.6 ± 5.8) were acquired from an anatomical donations program (Anatomical Gifts Registry, Hanover, MD). Two additional specimens from one additional donor were excluded from data processing due to a damaged and non-functional ACL. Methods of specimen preparation have been explicitly documented in previous literature (Bates et al., 2015; Boguszewski et al., 2011; Herfat et al., 2012b). Briefly, specimens were stored at -20 °C and thawed one day prior to testing. Specimens were resected of all soft tissue outside the knee joint capsule, leaving all intra-articular joint structures intact. A joint coordinate system was then defined using anatomical landmarks digitized with a coordinate measuring machine (Faro Digitizer F04L2, FARO Technologies, Inc., Lake Mary, FL) (Grood and Suntay, 1983). Custom mechanical fixtures then aligned and affixed the mechanical axes of the tibia with the primary axes of a 6-axis load cell (Theta Model; ATI

Industrial Automation, Apex, NC) that was mounted on the end effector of a six-degree-of-freedom (6-DOF) robotic arm (KR210; KUKA Robotics Corp., Clinton Township, MI). The femur was then fixed to a static table. This setup allowed the robotic manipulator to articulate the tibia around the femur as it simulated the recorded, *in vivo* kinematics about the knee joint center point (Bates et al., 2015; Boguszewski et al., 2011; Herfat et al., 2012b). Prior to simulation, each specimen was articulated to 45° flexion and 3 mm microminiature differential variable resistance transducers (DVRT, LORD MicroStrain, Inc., Williston, VT) were implanted parallel to fiber alignment just superior to the tibial insertion site on the anteromedial bundle of the ACL as well as on the MCL (Beynon et al., 1992; Levine et al., 2013). MCL insertion sites were distal to the femoral origin, midsubstance across the joint line, and proximal to the tibial insertion.

Initial limb orientation was different for each of the four simulated athletic tasks (male DVJ, male sidestep cutting, female DVJ, female sidestep cutting). For each task, initial limb position was matched to within 0.5° of the *in vivo* orientation that corresponded with initial ground contact for all three rotational DOFs. From this initial position, specimens were incrementally loaded in compression until a peak force of 2.0–2.5 bodyweights was achieved for DVJ simulations and 1.5–2.0 bodyweights was achieved for sidestep cutting simulations (Bates et al., 2013, 2015). Simulations were performed at room temperature and the joint was constantly hydrated with saline. All four motions were simulated on each specimen irrespective of specimen gender. Motions were mirrored to accommodate both right and left sides of each pair and identical kinematics pathways were articulated on each specimen. Prior to each simulation, specimens were run through 10 preconditioning cycles to minimize viscoelastic effects. After preconditioning, an additional 10 cycles were simulated where joint forces, joint torques, and ligament strains were recorded (Bates et al., 2015). Following the simulation of each *in vivo* recorded motion task, the robotic manipulator articulated each limb through isolated 4° rotations in each the internal, external, abduction, adduction, combined internal/abduction, and combined external/adduction DOFs. These limb articulations were performed relative to the initial contact orientation during landing for each motion task. This was done to assess ligament strain response relative to isolated knee rotations previously attributed to ACL injury risk (Hewett et al., 2005; Oh et al., 2012). After testing the knee was dissected down to the ligaments and the load cell was used to determine zero strain conditions based on the point of initial loading. In this isolated condition, where the ligament was the only structure transmitting force across the joint, the specimen was articulated back to initial contact orientation, compressed to an unloaded position, and slowly distracted until the force sensor first registered a constant distraction force. This location was determined to be the neutral strain position of the ligament, which allowed for the calculation of absolute ligament strain rather than strain relative to the DVRT insertion site. The remaining ligament was then resected and all simulations were repeated in a bone-only condition.

2.3. Data analysis

All forces and torques were analyzed in the tibial reference frame based on the knee joint coordinate system (Grood and Suntay, 1983). All torques are reported as internal joint moments. Forces and torques generated during the bone-only condition were subtracted from the intact knee simulations as they represent values generated from gravity and robot inertia (Boguszewski et al., 2011; Herfat et al., 2012b). All forces and torques were smoothed through a 12 Hz Fourier transform and translational forces were normalized to percent bodyweight. Further, all data was time normalized to percent of landing cycle. Instantaneous strain data was recorded by the DVRTs and at approximately 19 Hz and was interpolated to 101 points over the duration of landing phase. Landing cycle began at initial contact and ended when the minimum center of gravity was reached (Bates et al., 2013). To eliminate cycle effects, the 8th and 9th cycle of each simulation were used for data analysis. Descriptive statistics for asymmetry were identified by taking the absolute value of each variable after the difference between right and left limbs was calculated. Force/torque asymmetries were normalized to the range of values expressed in their respective DOF in order to provide perspective relative to the overall magnitude of loading at the joint. Force/torque asymmetries were also normalized to a magnitude of loading within their respective DOF that had been used in previous biomechanical testing to induce ACL failure. This reference magnitude was 268 N for antero-posterior loads, 80 N*m for internal-external torques, 112.7 N*m for flexion-extension torques, 150 N*m for abduction-adduction torques (Levine et al., 2013), 1195 N for medial-lateral loads (Mo et al., 2013), and 5100 N for compression-distraction loads (Meyer et al., 2008; Meyer and Haut, 2008). Paired t-tests were used to evaluate variables for statistical significance ($\alpha < 0.05$) between contralateral sides within each simulated task. Statistical analyses were performed in MATLAB using custom and built-in functions.

3. Results

3.1. Force torque outcomes

Force and torque outputs between contralateral pairs correlated well across all four simulated *in vivo* motion tasks (Figs. 1–4).

The magnitude of asymmetry between pairs was less than 30% of the overall range of force/torque measures in most degrees of freedom (Fig. 5). An exception to this was frontal plane torque where the average asymmetry was as high as $57.7 \pm 48.8\%$ of the total adduction range for a mean difference of $10.3 \pm 6.5 \text{ N}\cdot\text{m}$ between contralateral limbs. Further, within each DOF, the magnitude of asymmetry between sides was less than 10% of magnitude used to induce ACL structural failure in previous biomechanical investigations (Table 1). The only consistent exception to this pattern was posterior shear force, which exhibited asymmetries of up to 22.4% of the antero-posterior failure magnitude. The majority of force and torque metrics exhibited no significant differences between sides relative to initial contact and peak loading values (Table 2). The sole side-to-side asymmetry identified was peak adduction torque during the male cut motion, where the right limbs expressed larger moments than the left limbs ($P=0.04$).

3.2. Simulated motion strains

Initial contact and peak strains generated in the ACL and MCL from simulated *in vivo* tasks exhibited no significant side-to-side differences for any task ($P > 0.05$; Table 3). Mean asymmetry in peak ACL strain between sides was 4.0% and 4.6% for the simulated female and male DVJs, respectively (Table 3). There were no statistically significant differences in asymmetry magnitudes between the male and female simulations for both DVJs and sidestep cutting ($P > 0.05$). The overall range of strains in the ACL was greater on the right side than the left side specimens during female cut simulations ($P=0.02$). Conversely, overall strain range in the MCL was greater in the left side than right side specimens during male DVJ and male cut motions ($P < 0.02$).

3.3. Isolated rotation strains

None of the isolated rotations applied at any of the initial contact orientations induced statistically significant differences in ACL strain between leg sides ($P > 0.05$; Table 4). Similarly, none of the isolated rotations applied at any of the initial contact orientations induced statistically significant differences in MCL strain between leg sides ($P > 0.05$). There was only one statistically

significant difference between sides for the range of ligament strains created by opposing isolated rotations on the knee. Mean asymmetry in peak ACL strain between sides during the DVJ ranged from 2.64% (external rotation for the female) to 4.37% (abduction rotation for the male; Table 4). Mean asymmetry in peak MCL strain between sides during the DVJ ranged from 3.27% (combined adduction and external rotation for the female) to 4.65% (abduction rotation for the male; Table 4). For both sexes, pure abduction rotation produced the greatest magnitudes of strain asymmetry in both the ACL and MCL. For the both the DVJ and sidestep cutting tasks, there were no statistically significant differences between sexes relative to the magnitude of asymmetry generated by any of the applied 4° rotations ($P > 0.05$). The range of strain on the ACL created by isolated abduction and adduction rotations applied at the female DVJ orientation was greater for the left limb ($1.96 \pm 1.12\%$) than the right limbs ($1.23 \pm 0.73\%$; $P=0.01$). This was also true for the male sidestep cut orientation (left = $1.01 \pm 1.13\%$; right = $0.61 \pm 0.65\%$; $P=0.02$).

4. Discussion

The purpose of the present study was to determine if side-to-side asymmetries persist in biomechanical simulations, knowing that they exist during *in vivo* analysis of athletic movements. Contralateral limb pairs were used in *in vitro* simulations of *in vivo* athletic motions and compared for biomechanical differences. The present simulation controlled for bony positioning (through identical input kinematics) and external muscle loading on the joint (through the resection of soft tissue outside the joint capsule); therefore, any resultant differences would likely be attributed to geometrical variance between specimen anatomy. The data indicated that contralateral knee joints did not demonstrate statistical difference from one another during biomechanical *in vitro* tests.

The peak values obtained from the simulations analyzed in the current investigation are similar to those in previous studies. In a previous study, application of a 1600 N compression load to simulate a single-leg jump landing resulted in a peak force of $1680 \pm 380 \text{ N}$ (Withrow et al., 2006). The peak compression force in the present study for the male DVJ was $1694 \pm 903.8 \text{ N}$. Applying that 1600 N force to the lateral compartment of the knee

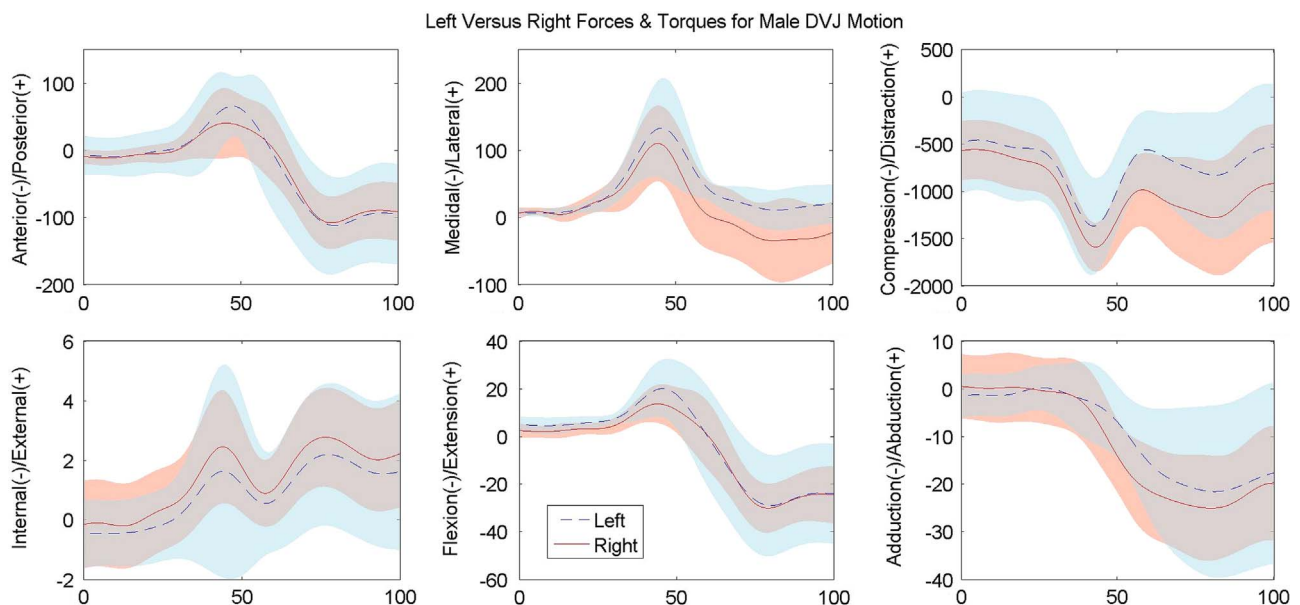


Fig. 1. The mean and standard deviation of internal knee forces and torques generated throughout landing phase during a simulated male DVJ for both the left (dashed) and right (solid) limb of a contralateral specimen pair.

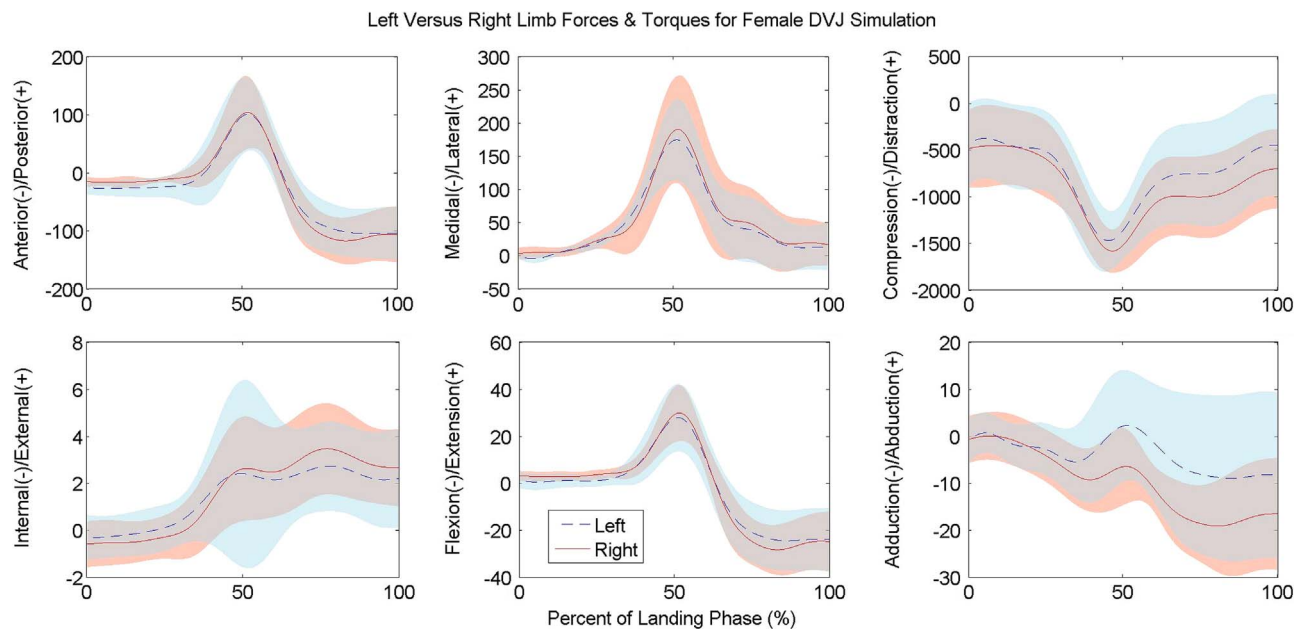


Fig. 2. Plots depicting the mean and standard deviation of internal knee forces and torques generated throughout landing phase during a simulated female DVJ for both the left (dashed) and right (solid) limb of a contralateral specimen pair.

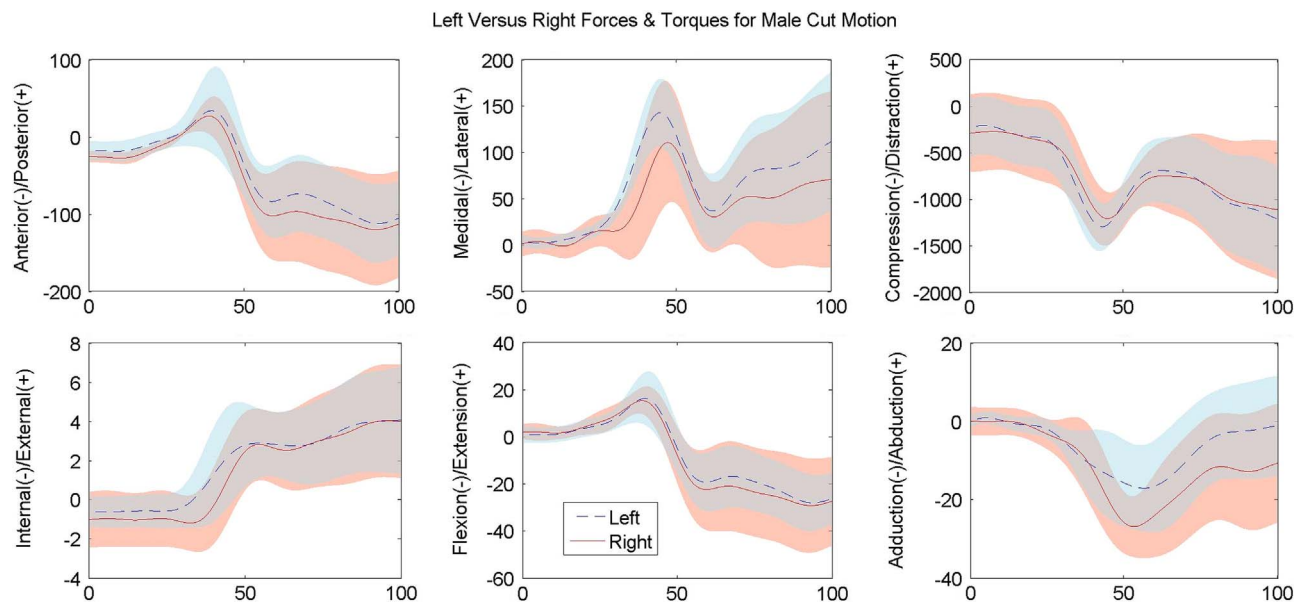


Fig. 3. Plots depicting the mean and standard deviation of internal knee forces and torques generated throughout landing phase during a simulated male DVJ for both the left (dashed) and right (solid) limb of a contralateral specimen pair.

to stimulate valgus loading during a single foot jump landing resulted in peak ACL valgus strain of $4.3 \pm 2.7\%$ (Withrow et al., 2006). In the present study, ACL abduction strain values range from 5.72% to 6.40% for the DVJ simulations. Another study showed that simulation of a single-leg jump landing involving a cut or pivot resulted in an average peak ACL strain of $5.4 \pm 3.7\%$ under internal tibial torque and $3.1 \pm 2.8\%$ externally (Oh et al., 2012). For the present study, peak ACL strains for the cut movement ranged from 3.90% to 8.32%. The ratios of ACL and MCL strains in the present study are consistent with an investigation that determined the ACL:MCL strain ratio for multi-planar loading mechanism is greater than 1.7 (Quatman et al., 2014).

There was an absence of significant mechanical differences between limb sides in biomechanical simulations, which supported the null hypothesis that side-to-side asymmetries would

not persist during *in vitro* tests. Similarly, absolute differences between sides were less than 10% of the magnitude recorded for ligament failure in five out of six DOFs. The one DOF that exceeded 10% of failure magnitude was posterior translation, which lacks relevance with respect to ACL failure. These findings suggested that contralateral knee joints should produce similar results and draw equivalent conclusions during biomechanical tests. In future *in vitro* simulations, specification of limb side should not be a dependent variable impacting the test results when input kinematics and external loads are universally controlled. Results of this study indicated that during *in vitro* simulation, specification of left or right knee joint does not significantly alter biomechanical outcomes during simulated athletic movements. This finding will help to further develop protocols for robotic simulation. It is therefore possible to use contralateral limbs interchangeably in

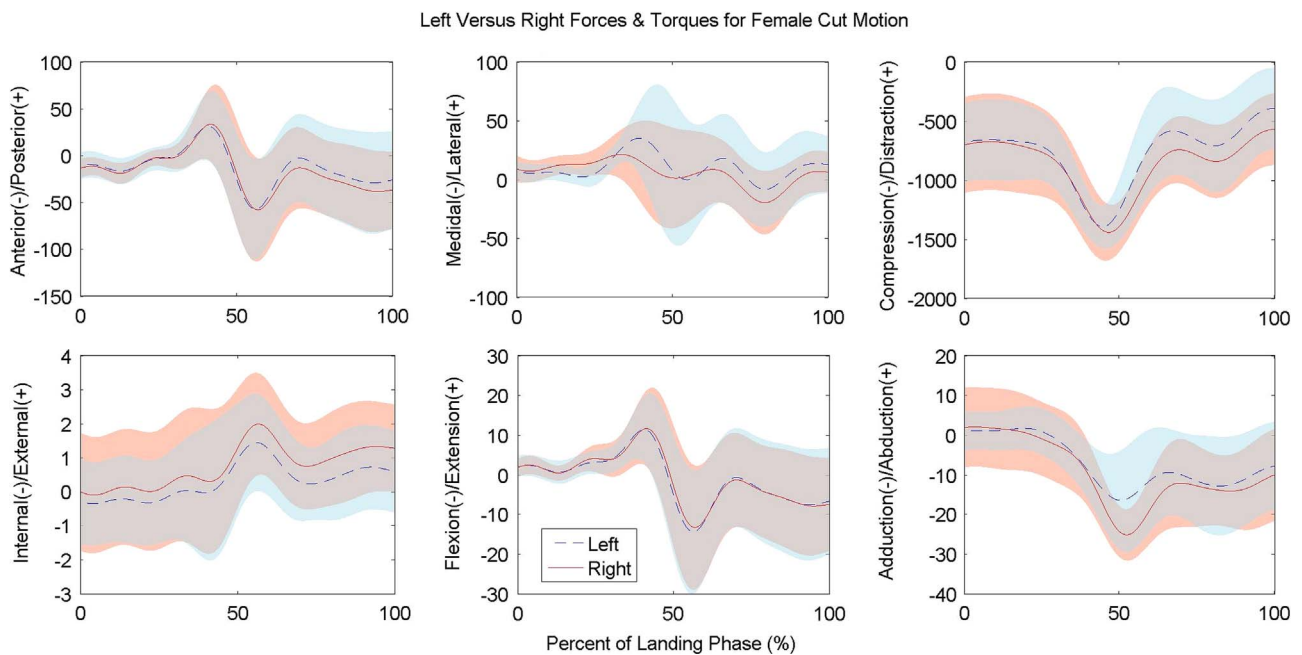


Fig. 4. Plots depicting the mean and standard deviation of internal knee forces and torques generated throughout landing phase during a simulated female DVJ for both the left (dashed) and right (solid) limb of a contralateral specimen pair.

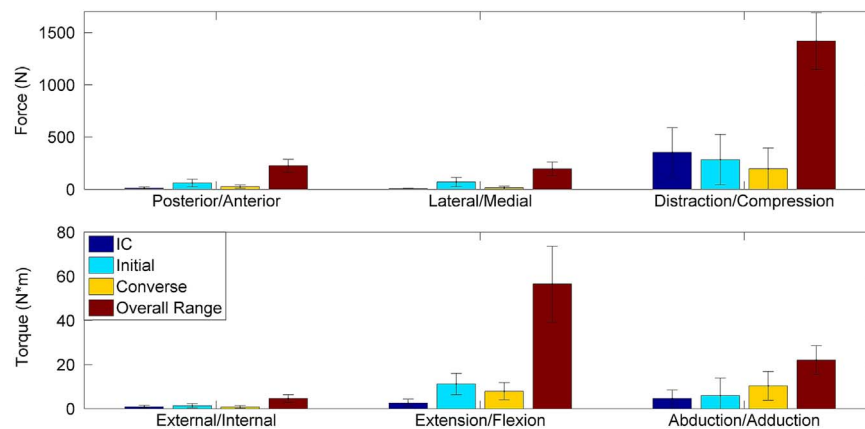


Fig. 5. For each DOF, bar plots (from left to right) depict joint loading asymmetry at the position of initial contact (IC); the position of peak loading magnitude in the direction initially listed for the given DOF; and the position of peak loading in the converse direction for the given DOF. The final (far right) column within each DOF represents the absolute range of loading expressed by the joint for that DOF throughout simulation. The data presented is from the female DVJ and is representative of trends observed in all four simulated tasks.

cadaveric simulations. Furthermore, direct comparisons can be made between structural behaviors in one knee and between its contralateral partner for isolated conditions. For example, an isolated ACL from a right knee can be compared to the isolated MCL from the respective left knee to gain a better understanding of the total knee's functional behavior.

Removal of a specimen and reinstallation for further testing resulted in clinically significant differences in test results (Goldsmith et al., 2014). Specifically, removal of the specimen setup hinders repeatability and reproducibility of biomechanical testing variables. That side-to-side variability between contralateral specimens expressed fewer statistical differences than repeated biomechanical testing on a single specimen following removal and reinstallation was surprising. The consistency of the present data between sides therefore reinforced the reproducibility of our previously published testing methodology and further validated the concept that right and left contralateral pairs can be used interchangeably in identical cadaveric simulations.

The one statistically significant side-to-side difference that was found relative to force and torque values was in the frontal plane. Adduction peak torque during the male sidestep cut task was found to be of greater magnitude in the right knee than the left. Movement in the frontal plane, specifically adduction and abduction, increases susceptibility to knee injury (Hewett et al., 2005; Toth and Cordasco, 2001). A sudden change of direction, simulated as the cutting motion in this study, is also identified to increase injury risk (Boden et al., 2000; Griffin et al., 2000; McNair et al., 1990; Mei et al., 2013). The male cut adduction peak torque difference is consistent with both of these identified risk factors. In addition, it has been reported that frontal plane kinematics are significantly higher in a cutting motion than in a hop landing task (Tanikawa et al., 2013). Additionally, unpublished data from our simulations have also shown that changes in frontal plane torques are particularly susceptible to $\pm 0.5^\circ$ alterations in the starting orientation. Therefore, there exists the possibility that the tolerance of the present setup protocol could have deviated the initial

Table 1
Mean magnitudes of force and torque asymmetries between contralateral limbs at IC and peak loading point for each DOF in the knee. Asymmetries are also normalized to percent of magnitude reported to induce failure during prior biomechanical testing for each DOF.

Failure Load		Female DVJ		Female Cut		Male DVJ		Male Cut	
		Asymmetry	% of Failure	Asymmetry	% of Failure	Asymmetry	% of Failure	Asymmetry	% of Failure
Force (N)									
A/P @ IC	268	12 ± 9	4.5%	5 ± 7	1.9%	17 ± 14	6.3%	10 ± 8	3.7%
Posterior	268	60 ± 36	22.4%	32 ± 14	11.9%	53 ± 33	19.8%	31 ± 25	11.6%
Anterior	268	26 ± 16	9.7%	17 ± 10	6.3%	39 ± 31	14.6%	40 ± 19	14.9%
M/L @ IC	1195	6 ± 5	0.5%	14 ± 6	1.2%	4 ± 3	0.3%	16 ± 7	1.3%
Lateral	1195	70 ± 43	5.9%	33 ± 40	2.8%	93 ± 61	7.8%	50 ± 77	4.2%
Medial	1195	15 ± 15	1.3%	27 ± 33	2.3%	39 ± 55	3.3%	22 ± 22	1.8%
C/D @ IC	5100	353 ± 237	6.9%	279 ± 187	5.5%	467 ± 172	9.2%	199 ± 110	3.9%
Distraction	5100	285 ± 240	5.6%	217 ± 149	4.3%	459 ± 189	9.0%	136 ± 63	2.7%
Compression	5100	196 ± 200	3.8%	132 ± 55	2.6%	200 ± 157	3.9%	98 ± 89	1.9%
Torque (N*m)									
I/E @ IC	80	0.9 ± 0.7	1.1%	0.9 ± 0.9	1.1%	0.9 ± 0.9	1.1%	0.7 ± 0.8	0.9%
External	80	1.3 ± 1.0	1.6%	0.8 ± 0.4	1.0%	1.1 ± 1.5	1.4%	1.2 ± 1.0	1.5%
Internal	80	0.8 ± 0.6	1.0%	0.8 ± 0.7	1.0%	0.9 ± 0.8	1.1%	1.0 ± 0.8	1.3%
F/E @ IC	112.7	2.6 ± 1.7	2.3%	1.4 ± 1.0	1.2%	3.4 ± 1.7	3.0%	2.0 ± 2.2	1.8%
Extension	112.7	11.2 ± 4.8	9.9%	6.7 ± 5.0	5.9%	12.8 ± 5.8	11.4%	9.2 ± 5.9	8.2%
Flexion	112.7	7.9 ± 3.9	7.0%	6.5 ± 4.5	5.8%	8.8 ± 7.1	7.8%	10.8 ± 7.3	9.6%
A/A @ IC	150	4.6 ± 3.9	3.1%	8.7 ± 7.3	5.8%	5.4 ± 3.7	3.6%	3.3 ± 3.3	2.2%
Abduction	150	5.9 ± 8.1	3.9%	8.8 ± 8.4	5.9%	6.7 ± 3.9	4.5%	4.8 ± 4.1	3.2%
Adduction	150	10.3 ± 6.5	6.9%	11.1 ± 10.2	7.4%	8.3 ± 6.6	5.5%	12.3 ± 7.8	8.2%

A/P=Anterior/Posterior, M/L=Medial/Lateral, C/D=Compression/Distraction, I/E=Internal/External, F/E=Flexion/Extension, A/A=Abduction/Adduction.

Reference failure loads obtained from Levine et al. (2013) (A/P, I/E, F/E, A/A), Mo et al. (2013) (M/L), and Meyer et al. (2008) (C/D). Translational force failure loads were uniaxially applied.

orientation enough to create small artifact differences in loading outcomes that propagated into statistical significance.

The ACL strain range was significantly different between limb sides during the female sidestep cut simulation. In the present study ACL strains at initial contact appeared to be slightly larger for the simulated female motion than the male tasks. Females tend to exhibit less knee flexion at initial contact; thus, they land in a more upright erect position than males, which increases the load on the ACL (Imwalle et al., 2009). Additionally, investigation of the effect of muscle contraction and tibial torques on ACL strain behavior has demonstrated that as knee flexion increased, ACL strain values gradually decreased (Fujiya et al., 2011; Renstrom et al., 1986). In the present simulations, the female motions began in a slightly more extended knee orientation than the male motions (Bates et al., 2015). Therefore, it is possible that the initial orientation of the female cut task placed greater load on the ACL and lead to greater initial strain values. Multiple retrospective studies suggest there is no significant relationship between side of injury and leg dominance (Matava, 2002; Negrete et al., 2007). There are mixed results about the relationship between gender and leg dominance on ACL injury. A study of subjects sustaining an ACL injury while playing soccer found 74.1% of males injured their dominant leg, whereas only 32% of females injured their dominant leg (Brophy et al., 2010). Other studies, however, have found no significant effect of gender on the relationship of ACL injury side and leg dominance (Matava, 2002; Negrete et al., 2007). Further investigation of gender and leg dominance effect on ACL injury may explain the difference in ACL strain range between limb sides found in the present study.

The MCL strain range was also significantly different between limb sides for half of the tasks simulated in the present study. The left limb MCL strain was consistently greater than the right limb. The MCL is the primary passive resistor to knee abduction (Boguszewski, 2012; Butler et al., 1980; Sankar et al., 2006). The MCL, however, is less critical than the ACL in stabilizing the knee, as established by the ACL: MCL strain ratio previously discussed (Quatman et al., 2014). It is known that approximately 90% of the general population is right side

dominant and that 67.74% of females injured their non-dominant leg (Brophy et al., 2010). MCL injuries are concomitant with ACL injuries 30% of cases (LaPrade et al., 2007; Sankar et al., 2006). These percentages may explain why the relative MCL strain was consistently greater in the left limb than the right limb in the present study.

A potential source for the limited magnitudes of asymmetry that were noted in this investigation lies in the specimen setup process. While the equipment used during setup is highly precise (Herfat et al., 2012a), and the process used to define the joint coordinate system is well established (Grood and Suntay, 1983), the initial preparation, fixturing, and mounting of the specimen is done by hand. Literature has shown that an alignment perturbation of 1 mm along the anterior-posterior axis can lead to ~50 N change in anterior force, while perturbation of 1 mm along the compression-distraction axis can lead to ~300 N change in compressive force throughout the robotic simulation of a gait cycle (Herfat et al., 2012a). These magnitudes happen to correspond with the magnitude of translational asymmetries in the present study. It is not unreasonable to speculate that initial alignment between contralateral pairs could deviate slightly and account for some of the magnitude of load asymmetry between sides. It should additionally be noted that rotational perturbations of 1° were not shown to impact either translational forces or rotational torques during simulation (Herfat et al., 2012a).

One limitation faced by the present study is the rate of simulation. Cycle duration of the in vitro simulation was approximately 2 s, while the duration of landing phase *in vivo* is approximately 0.2 s (Bates et al., 2013). Though rate of simulation will consequently affect rates of strain and loading within the joint, it has previously been proven that alterations to simulation rate from 10% to 100% loading rate do not influence peak values stiffness, modulus, failure load, or failure stress values within the patellar tendon (Blevins et al., 1994). Therefore, a reduced rate of simulation does not automatically indicate a corresponding reduced magnitude of loading in viscoelastic tissues. This limitation has previously been addressed in the literature (Boguszewski et al., 2011; Herfat et al., 2012a). Additionally, the current model is limited in that it does not account for specimen-specific geometry of

Table 2

Internal knee joint forces and torques generated during athletic task simulations. The values represent mean magnitude at initial contact (IC) as well as mean peak values for all degrees of freedom for both the left and right limb of a contralateral pair.

	Female DVJ		Male DVJ		Female Cut		Male Cut	
	Left	Right	Left	Right	Left	Right	Left	Right
Forces (N)								
Ant/Post @ IC	−25.00 ± 15.82	−15.71 ± 10.38	−7.43 ± 21.32	−9.57 ± 8.96	−10.71 ± 11.75	−13.71 ± 10.11	−18.29 ± 13.19	−25.71 ± 14.24
Posterior Peak	104.48 ± 68.59	106.35 ± 69.10	94.02 ± 60.41	58.64 ± 41.39	46.07 ± 32.31	39.70 ± 30.34	42.89 ± 37.44	29.68 ± 21.83
Anterior Peak	−119.99 ± 65.63	−122.88 ± 68.60	−128.14 ± 75.20	−110.42 ± 63.39	−65.34 ± 46.33	−65.15 ± 46.88	−116.04 ± 69.89	−128.76 ± 78.89
Med/Lat @ IC	0.29 ± 3.24	3.43 ± 6.13	8.29 ± 5.95	6.29 ± 6.62	7.29 ± 6.70	8.86 ± 9.12	4.71 ± 5.50	1.14 ± 9.16
Lateral Peak	177.77 ± 100.96	195.19 ± 114.70	134.55 ± 87.17	117.65 ± 73.91	46.24 ± 24.92	34.46 ± 23.49	151.79 ± 85.19	125.78 ± 80.44
Medial Peak	−11.96 ± 15.76	−6.82 ± 10.40	−4.46 ± 13.40	−43.07 ± 43.74	−21.53 ± 25.90	−29.58 ± 22.32	0.07 ± 5.87	−11.93 ± 20.40
Comp/Dist @ IC	−434.14 ± 384.40	−487.29 ± 378.54	−497.71 ± 461.78	−573.57 ± 365.96	−683.57 ± 426.71	−704.14 ± 457.27	−238.86 ± 252.31	−293.14 ± 320.30
Distraction Peak	−91.79 ± 202.93	−233.28 ± 188.41	−55.71 ± 238.43	−368.98 ± 278.12	−325.99 ± 265.66	−425.79 ± 281.42	−86.60 ± 126.75	−87.71 ± 107.89
Compression Peak	−1519.64 ± 820.85	−1642.52 ± 865.33	−1583.14 ± 856.01	−1694.91 ± 903.81	−1426.20 ± 750.90	−1453.75 ± 771.36	−1482.25 ± 783.65	−1530.65 ± 815.69
Torques (N°m)								
Int/Ext @ IC	−0.29 ± 0.69	−0.57 ± 0.73	−0.43 ± 0.83	−0.14 ± 1.00	−0.29 ± 0.90	0.00 ± 1.18	−0.57 ± 0.63	−1.00 ± 1.09
External Peak	4.07 ± 2.90	3.79 ± 2.35	3.40 ± 2.67	3.06 ± 1.94	1.59 ± 1.35	2.00 ± 1.45	4.32 ± 2.91	4.30 ± 2.85
Internal Peak	−0.71 ± 0.91	−0.65 ± 0.74	−0.77 ± 1.02	−0.37 ± 0.94	−0.69 ± 0.98	−0.30 ± 1.17	−0.90 ± 0.77	−1.55 ± 1.24
Flex/Ext @ IC	1.43 ± 2.52	3.14 ± 2.21	5.00 ± 3.47	2.43 ± 2.42	2.14 ± 2.19	1.86 ± 1.77	1.00 ± 2.47	2.14 ± 2.46
Extension Peak	28.15 ± 17.70	30.25 ± 17.58	23.59 ± 15.25	15.93 ± 9.96	12.08 ± 8.33	13.19 ± 8.68	17.14 ± 11.67	15.89 ± 8.90
Flexion Peak	−25.46 ± 15.90	−29.05 ± 16.57	−28.98 ± 21.21	−30.21 ± 17.16	−14.84 ± 13.09	−14.06 ± 12.37	−28.17 ± 16.90	−30.33 ± 20.52
Ab/Add @ IC	−1.00 ± 3.28	−0.71 ± 3.43	−1.57 ± 3.36	0.43 ± 4.63	0.86 ± 3.48	1.86 ± 6.88	0.14 ± 1.12	0.00 ± 2.48
Abduction Peak	5.81 ± 7.35	1.10 ± 3.19	2.81 ± 4.02	1.88 ± 4.97	2.88 ± 4.33	2.58 ± 6.80	5.29 ± 5.00	2.35 ± 2.44
Adduction Peak	−14.43 ± 11.46	−22.73 ± 12.80	−23.09 ± 16.20	−25.67 ± 15.03	−17.18 ± 12.02	−25.38 ± 13.86	−18.72 ± 11.87*	−28.74 ± 15.57*

* Indicates statistically significant difference between sides ($P < 0.05$).

Table 3

Mean ACL and MCL strain values and side to side asymmetries as recorded by DVRTs throughout each simulated task. Values were calculated for the left and right limbs of contralateral specimen pairs.

	Female DVJ			Male DVJ		
	Left	Right	Asymmetry	Left	Right	Asymmetry
ACL						
IC	4.24 ± 3.28%	4.43 ± 3.22%	3.05 ± 2.79%	3.34 ± 3.28%	3.16 ± 3.53%	4.80 ± 2.88%
Peak	7.27 ± 4.14%	6.33 ± 4.70%	4.00 ± 2.54%	7.67 ± 4.48%	6.33 ± 5.34%	4.60 ± 3.67%
Range	3.51 ± 2.63%	5.38 ± 4.12%	2.26 ± 3.11%	7.20 ± 4.49%	8.51 ± 5.11%	2.11 ± 2.51%
MCL						
IC	0.21 ± 1.69%	0.40 ± 2.96%	3.85 ± 3.23%	0.46 ± 1.77%	0.82 ± 3.15%	3.86 ± 3.84%
Peak	1.90 ± 1.71%	1.04 ± 3.25%	3.35 ± 2.79%	1.12 ± 1.62%	0.91 ± 3.15%	3.70 ± 3.48%
Range	1.76 ± 1.15%*	0.75 ± 0.55%*	1.03 ± 1.08%	0.95 ± 0.64%*	0.34 ± 0.27%*	0.61 ± 0.45%

* Indicates statistically significant difference between sides ($P < 0.05$).

Table 4

Mean ACL and MCL strains and side to side asymmetries generated by isolated 4° tibial rotations applied at the initial contact limb orientation in the specified degrees of freedom. Strains were calculated separately for the right and left limbs of each contralateral pair.

	Female DVJ			Male DVJ		
	Left	Right	Asymmetry	Left	Right	Asymmetry
ACL						
External	5.34 ± 3.41%	4.85 ± 3.21%	2.64 ± 2.17%	4.92 ± 3.36%	4.42 ± 3.61%	3.78 ± 2.51%
Internal	4.12 ± 3.17%	3.94 ± 2.94%	2.61 ± 2.31%	4.12 ± 3.25%	2.83 ± 3.23%	3.71 ± 2.28%
Abduction	6.40 ± 4.05%	6.14 ± 3.82%	3.61 ± 2.44%	5.92 ± 4.11%	5.72 ± 3.94%	4.37 ± 2.84%
Adduction	5.85 ± 3.71%	5.61 ± 3.63%	3.66 ± 2.39%	5.19 ± 3.62%	4.93 ± 3.77%	4.11 ± 2.75%
Abduction & Internal	6.64 ± 4.01%	6.08 ± 3.83%	3.35 ± 2.62%	6.36 ± 4.08%	6.04 ± 4.08%	4.15 ± 2.92%
Adduction & External	5.05 ± 3.33%	4.98 ± 3.53%	3.27 ± 2.32%	4.58 ± 3.32%	3.99 ± 3.66%	3.85 ± 2.46%
MCL						
External	−0.01 ± 1.58%	0.36 ± 3.12%	3.80 ± 3.24%	0.26 ± 1.57%	0.72 ± 3.18%	3.78 ± 3.67%
Internal	−0.03 ± 1.51%	0.27 ± 3.11%	3.77 ± 3.17%	0.18 ± 1.63%	0.66 ± 3.21%	3.70 ± 3.85%
Abduction	1.47 ± 2.29%	1.66 ± 3.74%	4.45 ± 4.41%	1.82 ± 2.57%	1.99 ± 3.90%	4.65 ± 4.64%
Adduction	−0.60 ± 1.56%	−0.60 ± 2.82%	3.46 ± 3.03%	−0.46 ± 1.68%	−0.18 ± 2.92%	3.53 ± 3.63%
Abduction & Internal	1.56 ± 1.96%	1.50 ± 3.66%	4.04 ± 4.19%	1.89 ± 2.29%	1.81 ± 3.79%	4.35 ± 4.52%
Adduction & External	−1.05 ± 1.54%	−1.12 ± 2.76%	3.27 ± 2.83%	−0.93 ± 1.74%	−0.57 ± 2.78%	3.69 ± 3.20%

*Indicates statistically significant difference between sides ($P < 0.05$).

the cadaveric limbs. While, previous application has demonstrated that the present model exhibits excellent inter-specimen loading reliability in all six DOFs, this limitation is expected to attribute to some of the relatively larger standard deviations presently reported (Bates et al., 2015). Another potential limitation is that for *in vivo* studies, each limb has separate, unique kinematics. There are known differences between dominant and non-dominant limb sides *in vivo* (Lanshammar and Ribom, 2011). However, the specimen population in this study could not be separated by limb dominance because the information was not provided for each donor. Therefore, only one side was chosen for simulation in this study, which was applied to both limbs of the contralateral pair. Therefore, it should be noted that the present study was not an investigation of side-to-side differences as they would occur *in vivo*, but an investigation of asymmetries that arise when contralateral limbs are run through identical *in vitro* test protocols. The present study determined if anatomical geometry between limbs results in mechanical differences during simulation, not if the effects of limb dominance on kinematics result in mechanical differences. As documented in the literature, the translational kinematic input for this model was unified rather than specimen specific (Bates et al., 2015). While a limitation to this model, skin based 3D motion capture is known to demonstrate translational artifact errors that may be larger in magnitude than the actual ROM traversed by the joint (Benoit et al., 2006; Miranda et al., 2013). Individual translational inputs derived from each *in vivo* subject would present additional opportunities for these

errors to confound and degrade the present model. Thus, uniform kinematics inputs were utilized for the translations DOFs. Further, *in vivo* there would be varying muscle activations between trials; however, this factor of external loading on the joint was controlled for in the present simulation, which consequently reduced the natural intra-specimen loading variability that is observed between trials *in vivo* (Bates et al., 2015; Ford et al., 2007).

Utilization of *in vivo* athletic kinematics to drive *in vitro*, robotically-manipulated biomechanical simulations revealed general absence of significant asymmetry between contralateral limb pairs. The data suggested that when biomechanical simulations are performed, limb sides can be used interchangeably. Similarly, when contralateral limbs from the same donor are run through the same simulation protocol, their outcome measures must be averaged into a single data point as to not confound the results. Further, the similarities in outcomes between contralateral sides indicated that it is possible to make direct, reliable statistical comparisons of separate test protocols applied to opposite sides of the same contralateral pair. This concept is useful when proposed test methodologies are destructive to the specimen, such as in injury simulations.

Conflict of interest

We declare that we have no conflicts of interest in the authorship or publication of this contribution.

Acknowledgements

This work was supported by the National Institutes of Health/NIAMS Grants #R01-AR049735, #R01-AR055563, #R01-AR056660 and #R01-AR056259. The authors would also like to acknowledge the support of the staff at the Biodynamics Lab at Mayo Clinic, the Sports Health and Performance Institute at the Ohio State University and the Sports Medicine Biodynamics Laboratory at Cincinnati Children's Hospital.

References

- Arendt, E.A., Agel, J., Dick, R., 1999. Anterior cruciate ligament injury patterns among collegiate men and women. *J. Athl. Train.* 34, 86–92.
- Bates, N.A., Ford, K.R., Myer, G.D., Hewett, T.E., 2013. Impact differences in ground reaction force and center of mass between the first and second landing phases of a drop vertical jump and their implications for injury risk assessment. *J. Biomech.* 46, 1237–1241.
- Bates, N.A., Nesbitt, R.J., Shearn, J.T., Myer, G.D., Hewett, T.E., 2015. A novel methodology for the simulation of athletic tasks on cadaveric knee joints with respect to in vivo kinematics. *Ann. Biomed. Eng.* 43, 2456–2466.
- Benoit, D.L., Ramsey, D.K., Lamontagne, M., Xu, L., Wretenberg, P., Renstrom, P., 2006. Effect of skin movement artifact on knee kinematics during gait and cutting motions measured in vivo. *Gait Posture* 24, 152–164.
- Beynon, B., Howe, J.G., Pope, M.H., Johnson, R.J., Fleming, B.C., 1992. The measurement of anterior cruciate ligament strain in vivo. *Int. Orthop.* 16, 1–12.
- Blevins, F.T., Hecker, A.T., Bigler, G.T., Boland, A.L., Hayes, W.C., 1994. The effects of donor age and strain rate on the biomechanical properties of bone-patellar tendon-bone allografts. *Am. J. Sports Med.* 22, 328–333.
- Boden, B.P., Dean, G.S., Feagin, J.A., Garrett, W.E., 2000. Mechanisms of anterior cruciate ligament injury. *Orthopedics* 23, 573–578.
- Boguszewski, D.V., 2012. Characterizing the Porcine Knee as a Biomechanical Surrogate Model of the Human Knee to Study the Anterior Cruciate Ligament (Ph.D. Dissertation). University of Cincinnati, Cincinnati, OH, USA.
- Boguszewski, D.V., Shearn, J.T., Wagner, C.T., Butler, D.L., 2011. Investigating the effects of anterior tibial translation on anterior knee force in the porcine model: is the porcine knee ACL dependent? *J. Orthop. Res.* 29, 641–646.
- Brophy, R., Silvers, H.J., Gonzales, T., Mandelbaum, B.R., 2010. Gender influences: the role of leg dominance in ACL injury among soccer players. *Br. J. Sport. Med.* 44, 694–697.
- Butler, D.L., Noyes, F.R., Grood, E.S., 1980. Ligamentous restraints to anterior-posterior drawer in the human knee. A biomechanical study. *J. Bone Jt. Surg. Am.* 62, 259–270.
- Di Stasi, S.L., Logerstedt, D., Gardinier, E.S., Snyder-Mackler, L., 2013. Gait patterns differ between ACL-reconstructed athletes who pass return-to-sport criteria and those who fail. *Am. J. Sports Med.* 41, 1310–1318.
- Ford, K.R., Myer, G.D., Hewett, T.E., 2003. Valgus knee motion during landing in high school female and male basketball players. *Med. Sci. Sports Exerc.* 35, 1745–1750.
- Ford, K.R., Myer, G.D., Hewett, T.E., 2007. Reliability of landing 3D motion analysis: implications for longitudinal analyses. *Med. Sci. Sports Exerc.* 39, 2021–2028.
- Ford, K.R., Myer, G.D., Toms, H.E., Hewett, T.E., 2005. Gender differences in the kinematics of unanticipated cutting in young athletes. *Med. Sci. Sport. Exerc.* 37, 124–129.
- Fujiya, H., Goto, K., Kohn, T., Aoki, H., 2011. Changes of SM muscles after STG harvest. *Int. J. Sport. Med.*
- Goldsmith, M.T., Smith, S.D., Jansson, K.S., LaPrade, R.F., Wijdicks, C.A., 2014. Characterization of robotic system passive path repeatability during specimen removal and reinstallation for in vitro knee joint testing. *Med. Eng. Phys.* 36, 1331–1337.
- Griffin, L.Y., Agel, J., Albohm, M.J., Arendt, E.A., Dick, R.W., Garrett, W.E., Garrick, J.G., Hewett, T.E., Huston, L., Ireland, M.L., Johnson, R.J., Kibler, W.B., Lephart, S., Lewis, J.L., Lindenfeld, T.N., Mandelbaum, B.R., Marchak, P., Teitz, C.C., Wojtys, E.M., 2000. Noncontact anterior cruciate ligament injuries: risk factors and prevention strategies. *J. Am. Acad. Orthop. Surg.* 8, 141–150.
- Griffin, L.Y., Albohm, M.J., Arendt, E.A., Bahr, R., Beynon, B.D., Demaio, M., Dick, R.W., Engebretsen, L., Garrett, W.E., Jr., Hannafin, J.A., Hewett, T.E., Huston, L.J., Ireland, M.L., Johnson, R.J., Lephart, S., Mandelbaum, B.R., Mann, B.J., Marks, P.H., Marshall, S.W., Myklebust, G., Noyes, F.R., Powers, C., Shields, C., Jr., Shultz, S.J., Silvers, H., Slaughterbeck, J., Taylor, D.C., Teitz, C.C., Wojtys, E.M., Yu, B., 2006. Understanding and preventing noncontact anterior cruciate ligament injuries: a review of the Hunt Valley II meeting. *Am. J. Sports Med.* 34, 2005, 1512–1532.
- Grood, E.S., Suntay, W.J., 1983. A joint coordinate system for the clinical description of three dimensional motions: application to the knee. *J. Biomech. Eng.* 105, 136–144.
- Herfat, S.T., Boguszewski, D.V., Nesbitt, R.J., Shearn, J.T., 2012a. Effect of perturbing a simulated motion on knee and anterior cruciate ligament kinetics. *J. Biomech. Eng.* 134, 104504.
- Herfat, S.T., Boguszewski, D.V., Shearn, J.T., 2012b. Applying simulated in vivo motions to measure human knee and ACL kinetics. *Ann. Biomed. Eng.* 40, 1545–1553.
- Hewett, T.E., Lindenfeld, T.N., Riccobene, J.V., Noyes, F.R., 1999. The effect of neuromuscular training on the incidence of knee injury in female athletes. A prospective study. *Am. J. Sports Med.* 27, 699–706.
- Hewett, T.E., Myer, G.D., Ford, K.R., Heidt Jr., R.S., Colosimo, A.J., McLean, S.G., van den Bogert, A.J., Paterno, M.V., Succop, P., 2005. Biomechanical measures of neuromuscular control and valgus loading of the knee predict anterior cruciate ligament injury risk in female athletes: a prospective study. *Am. J. Sports Med.* 33, 492–501.
- Imwalle, L.E., Myer, G.D., Ford, K.R., Hewett, T.E., 2009. Relationship between hip and knee kinematics in athletic women during cutting maneuvers: a possible link to noncontact anterior cruciate ligament injury and prevention. *J. Strength Cond. Res.* 23, 2223–2230.
- Johnson, D.L., Warner, J.P., 1993. Diagnosis for anterior cruciate ligament surgery. *Clin. Sports Med.* 12, 671–684.
- Lanshammar, K., Ribom, E.L., 2011. Differences in muscle strength in dominant and non-dominant leg in females aged 20–39 years – a population-based study. *Phys. Ther.* 12, 76–79.
- LaPrade, R.F., Wentorf, F.A., Fritts, H., Gundry, C., Hightower, C.D., 2007. A prospective magnetic resonance imaging study of the incidence of posterolateral and multiple ligament injuries in acute knee injuries presenting with a hemarthrosis. *Arthroscopy* 23, 1341–1347.
- Levine, J.W., Kiapour, A.M., Quatman, C.E., Wordeman, S.C., Goel, V.K., Hewett, T.E., Demetropoulos, C.K., 2013. Clinically relevant injury patterns after an anterior cruciate ligament injury provide insight into injury mechanisms. *Am. J. Sports Med.* 41, 385–395.
- Matava, M.J., 2002. Limb dominance as a potential etiologic factor in noncontact anterior cruciate ligament tears. *J. Knee Surg.* 15, 11.
- McNair, P.J., Marshall, R.N., Matheson, J.A., 1990. Important features associated with acute anterior cruciate ligament injury. *N.Z. Med. J.* 103, 537–539.
- Mei, Y., Ao, Y.F., Wang, J.-Q., Ma, Y., Zhang, X., Wang, J.-N., Zhu, J.-X., 2013. Clinical characteristics of 4355 patients with anterior cruciate ligament injury. *Chin. Med. J.* 126, 4487–4492.
- Meyer, E.G., Baumer, T.G., Slade, J.M., Smith, W.E., Haut, R.C., 2008. Tibiofemoral contact pressures and osteochondral microtrauma during anterior cruciate ligament rupture due to excessive compressive loading and internal torque of the human knee. *Am. J. Sports Med.* 36, 1966–1977.
- Meyer, E.G., Haut, R.C., 2008. Anterior cruciate ligament injury induced by internal tibial torsion or tibiofemoral compression. *J. Biomech.* 41, 3377–3383.
- Miranda, D.L., Rainbow, M.J., Crisco, J.J., Fleming, B.C., 2013. Kinematic differences between optical motion capture and biplanar videoradiography during a jump-cut maneuver. *J. Biomech.* 46, 567–573.
- Mo, F., Arnoux, P.J., Zahidi, O., Masson, C., 2013. Injury thresholds of knee ligaments under lateral-medial shear loading: an experimental study. *Trauma Inj. Prev.* 14, 623–629.
- Negrete, R.J., Schick, E.A., Cooper, J.P., 2007. Lower-limb dominance as a possible etiologic factor in noncontact anterior cruciate ligament tears. *J. Strength Cond. Res.* 21, 270–273.
- Oh, Y.K., Kreinbrink, J.L., Wojtys, E.M., Ashton-Miller, J.A., 2012. Effect of axial tibial torque direction on ACL relative strain and strain rate in an in vitro simulated pivot landing. *J. Orthop. Res.* 30, 528–534.
- Pappas, E., Carpes, F.P., 2012. Lower extremity kinematic asymmetry in male and female athletes performing jump-landing tasks. *J. Sci. Med. Sport* 15, 87–92.
- Pappas, E., Zampeli, F., Xergia, S.A., Georgoulis, A.D., 2013. Lessons learned from the last 20 years of ACL-related in vivo-biomechanics research of the knee joint. *Knee Surg. Sport. Traumatol. Arthrosc.* 21, 755–766.
- Paterno, M.V., Ford, K.R., Myer, G.D., Heyl, R., Hewett, T.E., 2007. Limb asymmetries in landing and jumping 2 years following anterior cruciate ligament reconstruction. *Clin. J. Sport Med.* 17, 258–262.
- Quatman, C.E., Kiapour, A.M., Demetropoulos, C.K., Kiapour, A., Wordeman, S.C., Levine, J.W., Goel, V.K., Hewett, T.E., 2014. Preferential loading of the ACL compared with the MCL during landing: a novel in sim approach yields the multiplanar mechanism of dynamic valgus during ACL injuries. *Am. J. Sports Med.* 42, 177–186.
- Renstrom, P., Arms, S.W., Stanwyck, T.S., Johnson, R.J., Pope, M.H., 1986. Strain within the anterior cruciate ligament during hamstring and quadriceps activity. *Am. J. Sports Med.* 14, 83–87.
- Renstrom, P.A., 2013. Eight clinical conundrums relating to anterior cruciate ligament (ACL) injury in sport: recent evidence and a personal reflection. *Br. J. Sports Med.* 47, 367–372.
- Sankar, W.N., Wells, L., Sennett, B.J., Wiesel, B.B., Ganley, T.J., 2006. Combined anterior cruciate ligament and medial collateral ligament injuries in adolescents. *J. Pediatr. Orthop.* 26, 733–736.
- Tanikawa, H., Matsumoto, H., Komiya, I., Kiriya, Y., Toyama, Y., Nagura, T., 2013. Comparison of knee mechanics among risky athletic motion for non-contact anterior cruciate ligament injury. *J. Appl. Biomech.* 29, 749–755.
- Toth, A.P., Cordasco, F.A., 2001. Anterior cruciate ligament injuries in the female athlete. *J. Gen. Specif. Med.* 4, 25–34.
- Withrow, T.J., Huston, L.J., Wojtys, E.M., Ashton-Miller, J.A., 2006. The effect of an impulsive knee valgus moment on in vitro relative ACL strain during a simulated jump landing. *Clin. Biomech.* 21, 977–983.